Submicron ionography of nanostructures using a femtosecond-laser-driven-cluster-based source

A. Ya. Faenov,[1,2,a] T. A. Pikuz,[1,2] Y. Fukuda,[1,3] M. Kando,[1] H. Kotaki,[1] T. Homma,[1] K. Kawase,[1] T. Kameshima,[1] A. Pirozhkov,[1,3] A. Yogo,[1,3] M. Tampo,[1,3] M. Mori,[1] H. Sakaki,[1,3] Y. Hayashi,[1] T. Nakamura,[1] S. A. Pikuz, Jr.,[2] I. Yu. Skobelev,[2] S. V. Gasilov,[2] A. Giulietti,[4] C. A. Cecchetti,[4] A. S. Boldarev,[5] V. A. Gasilov,[5] A. Magunov,[6] S. Kar,[7] M. Borghesi,[7] P. Bolton,[1,3] H. Daido,[1,3] T. Tajima,[1,3] Y. Kato,[8] and S. V. Bulanov[1,3,6]

[1]*Kansai Photon Science Institute and Photo-Medical Research Center, JAEA, Kyoto 619–0215, Japan*
[2]*Joint Institute for High Temperatures, RAS, Moscow 125412, Russia*
[3]*Photo-Medical Research Center, JAEA, Kizugawa-city, Kyoto 619-0215, Japan*
[4]*ILIL-Istituto per i Processi Chimico-Fisici, CNR, Pisa 56124, Italy*
[5]*M.V. Keldysh Institute of Applied Mathematics, RAS 125047, Russia*
[6]*A. M. Prokhorov Institute of General Physics, RAS, Moscow 125407, Russia*
[7]*The Queen's University of Belfast, Belfast BT7 INN, United Kingdom*
[8]*The Graduate School for the Creation of New Photonics Industries, Hamamatsu 431–1202, Japan*

(Received 5 March 2009; accepted 30 July 2009; published online 9 September 2009)

An intense isotropic source of multicharged carbon and oxygen ions with energy above 300 keV and particle number $>10^8$ per shot was obtained by femtosecond Ti:Sa laser irradiation of submicron clusters. The source was employed for high-contrast contact ionography images with 600 nm spatial resolution. A variation in object thickness of 100 nm was well resolved for both Zr and polymer foils. © *2009 American Institute of Physics*. [doi:10.1063/1.3210785]

The development of methods and tools for imaging and diagnosis of low-contrast objects with submicron resolution is an important aim for the purposes of material science, medicine, and nanoindustry. One of such promising imaging methods is the ionography technique using protons or multicharged ions produced by short, intense laser pulse irradiation of solid targets.[1–3] In a stopping radiography mode, the best contrast and spatial resolution of proton or ion images will be provided if the stopping range of the probing particles exceeds slightly the thickness of the analyzed sample and the sample is placed in contact with detector. With such an arrangement, particles with relatively low (some hundreds keV) energies could be used effectively for imaging of ultrathin materials. One of the most promising approaches for production of multicharged ions with some hundreds keV energies is the utilization of femtosecond laser pulses coupled with gas cluster targets.[4] In this paper, we present the results of experiments using femtosecond-laser-driven-cluster-based plasma as a source of multicharged ions with some hundreds keV energies for contact submicron imaging of low contrast ultrathin foils and biological objects. Modeling of ion imaging of 100 nm Zr foils supports our experimental results.

The experiments were carried out at the Kansai Photon Science Institute JAEA (Japan) on the JLITE-X facility. Ti:sapphire laser pulses with 36 fs duration and 120 mJ energy were focused by a parabolic mirror to a 50 μm diameter spot, giving a focused intensity of 3×10^{17} W/cm^2. The target consisted of gas clusters created by the injection of 60 bar supersonic jet to the vacuum through a specially developed nozzle.[5] The gas employed was a mixture of 90% He +10% CO_2, which provides the generation of 0.5 μm CO_2 clusters.[6] Both theoretical and experimental optimization was carried out in order to increase the size of clusters, laser beam contrast, and to select optimum focusing position of laser beam as the brightness and energy distribution of ion source strongly depended from all of these parameters. The laser pulse was focused on the jet axis at a distance of 1.5 mm from the nozzle [Fig. 1(a)]. The parameters of the laser plasma and the energy distributions of the fast ions were measured by means of high resolution x-ray Focusing Spectrometer with Spatil Resolution (FSSR) (1) and (2) spectrometers[6,7] based on spherically bent mica crystals, which were set, respectively, parallel and perpendicular to the laser beam propagation at a distance of 220 mm from the

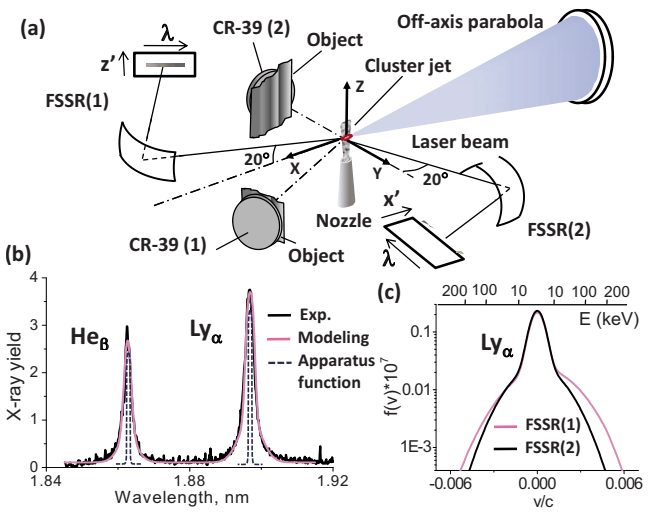

FIG. 1. (Color online) (a) Experimental setup. (b) Traces in the most broadening part of spectral lines of He- and H-like ions of oxygen, observed in the direction of laser beam propagation, and their modeling using the following plasma parameters: $N_e=10^{20}$ cm^{-3}, $T_e=110$ eV, $T_{i,bulk}=3$ keV, $T_{i,fast}=60$ keV. (c) One-dimensional velocity distribution function extracted from experimental spectra of He$_\beta$ and Ly$_\alpha$ lines of oxygen ions.

[a]Electronic mail: faenov.anatoly@jaea.go.jp.

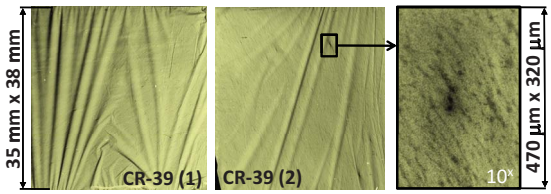

FIG. 2. (Color online) Ionography images of 1 um polypropylene foils obtained on different observation direction to ion source. Magnified part of image demonstrated that single micron-size inhomogeneous inclusions in polypropylene foils are clearly resolved.

target and at a 20° angle above the laser beam axis. The first reflection order of the crystal was used to observe He_β and Ly_α spectral lines of He- and H-like oxygen multicharged ions [Fig. 1(b)].

The objects to be imaged by ionography were situated at distances of 140 and 160 mm from the laser target, at different observation angles to the laser beam axis [Fig. 1(a)]. The fast ions generated in the plasma propagated through the imaging object and were stopped in the polymer dosimeter film CR-39, positioned in contact with the object's back surface. We selected CR39 film as a detector for high-resolution ionography imaging due to the fact that it not only provides high spatial resolution and also a sensitive and precise flux measurement, but it has also the advantage of having no protective layer, an important requirement for the detection of low energy ions (in our case only 100–500 keV). Following 15 min chemical etching of the CR-39 film, the latent track of every absorbed fast particle is revealed as a channel with cross section ~0.2 μm and longitudinal size ~1 μm, depending on fast particle energy. After etching, the images are registered by an optical microscope, which determines the spatial resolution ~0.3 μm of the technique. Diagnosis of the plasma parameters was carried out with the use of the relative intensities of the x-ray spectral lines, while the energy distribution of fast ions was determined from the analysis of spectral line profiles according to the method described in Ref. 7. The plasma parameters and ion energy distribution inferred from these spectra are presented in Fig. 1 and demonstrated that H- and He-like O^{+6} and O^{+7} ions were accelerated quite isotropically. The isotropy rate of the generated ion flux, the sensitivity of the ionography method to different thickness, and density of objects and the possibility to achieve submicron spatial resolution were investigated. Both images on the surface of CR-39 detector covered by a 1 μm polypropylene film, obtained along different lines of sight from the plasma source, have uniform background on the whole areas (Fig. 2). This confirms that the cluster-based laser plasma source produces enough isotropic, homogeneous ion flux in the full solid angle with the total number $>10^8$ ions per laser shot. Based on the fact that the effective thickness of the foil along the probe ion propagation in correspondence to foil wrinkles will vary less than 100 nm, we can deduce that the proposed ionography method has sensitivity to the target thickness in the order of 100 nm even for objects composed of light chemical elements (C and H). In order to ensure that the obtained images were formed by multicharged oxygen or carbon ions, Thomson parabolas (not shown in Fig. 1) were set up in some shots, at distances and directions close to the CR-39 detectors. The results obtained show that carbon and oxygen ions with charges from +1 to +4 and energies upto 4 MeV were generated in our

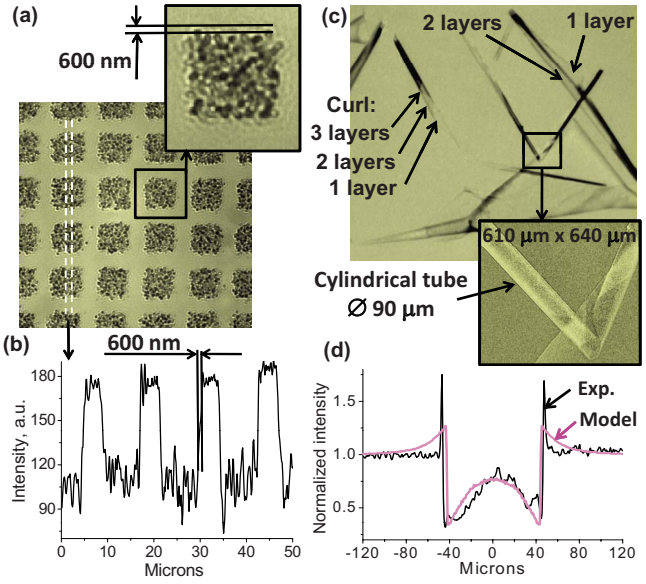

FIG. 3. (Color online) The image (a) and the trace (b) of 2000 lpi mesh consisted from separate latent tracks, produced by ions penetrated through the open parts of mesh and recorded in CR-39. Sharpness of edge slope demonstrates spatial resolution ~600 nm. (c) Image of damaged Zr 100 nm foil, self-shaped to swirls and tubes. The areas of multiple layers superimpose are recognized. (d) Comparison of intensity of image modeled with assumption of oxygen ions distribution with T_{ion}=60 keV and experimental intensities of Zr 90 μm tube.

experiments.[8] No evidence for protons or He ions has been obtained. Additional control experiments when we have used pure He gas expanding in the same nozzle, demonstrated no images on the CR-39 detectors. We could therefore conclude that the images, obtained on CR-39 films have been formed only by oxygen and carbon fast ions, produced in CO_2 clusters target. Using SRIM (Ref. 9) modeling, we estimated that the energy of such ions required to pass through polypropylene film with 1 μm thickness and form contrast image must be in the range of 250–500 keV. In a further experiment, the images of two-dimensional 2000 lpi mesh made of 5 μm Cu wires were obtained [Fig. 3(a)]. The magnification of the image of a single empty mesh cell (Fig. 3) shows that it consists of overlapping pits representing etched latent tracks of fast ions in CR-39. We used traditional optical approach for estimation of the image spatial resolution by sharpness of the edge of the image slope and obtained ~600 nm value [Fig. 3(b)]. The probing ion flux is uniform across an area of tens of mm dimension, leading to an imaging setup with field-of-view/spatial resolution ratio of the order of 10^5. In order to demonstrate that foils with nanoscale thickness could be resolved by the ionography technique, the image of 100 nm zirconium foils was obtained and is shown in Fig. 3(c). Damaged portions of the Zr foil, which curl up to tubes and swirls, are clearly resolved. A simulation for the Zr tube radiograph was carried out employing the MPRM code[3] based on the SRIM Monte-Carlo simulation package.[9] An oxygen beam with polychromatic ion energies, determined from x-ray measurements with ions temperature of 60 keV, was used as the particle probe and passed through investigated object the particle number density across the detector was reconstructed. A profile in good agreement with the experimental lineout, as shown in the Fig. 3(d), is obtained by the simulation for a Zr tube of 90 μm diameter and 100 nm thicknesses, with the detector placed at 10 μm distance from

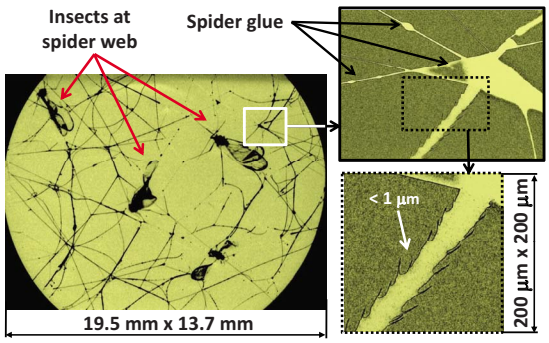

FIG. 4. (Color online) Ionography image of spider web structure with silk, glue drops, and insects caught on it. The setae of the insect with size ~1 μm extremity are perfectly resolved in magnified part of image.

the sample. Additional modeling with 50 and 100 μm distances between sample and detector shows that the contrast of Zr images practically does not change. So, we can conclude that the developed method of ionography is suitable for nanostructure diagnostics and measurements of thickness inhomogeneities smaller than 100 nm. In a further series of measurements, the microscopic image of a spider web with various insects embedded in it was obtained (Fig. 4). The magnified area of the image allows to distinguish fine details and to measure the thickness of the spider web, as well as drops of biological glue on it, and also to resolve the insect structures with <1 μm spatial resolution.

It is necessary to note that using relatively low ion energies such as in the present work the role of the collisions with the target atom nuclei plays an increasingly important role in the stopping process. Due to close collisions, the incident ions can deflect on wide angles that leads to an increased spatial divergence of the ion flux passed through the object being imaged. This effect results in a reduction of spatial resolution of the imaging. It follows that in order to minimize image quality degradation due to scattering effect it is imperative to place the detector in contact with the back surface of an object.

In conclusion we demonstrated that easy production of large numbers of different sub-MeV ion species emitted in a highly isotropic fashion, places femtosecond–laser-driven-cluster-based plasma as a bright multicharged ions source particularly well suited for submicron ionography. This technique can provide an advanced diagnostic tool for precise measurements of thickness, density, and structure in low contrast and nanoscale objects.

This work was partly supported by the Japan MEXT Grant-in-Aid for Kiban Grant No. A _20244065, by the Special Coordination Fund for Promoting Science and Technology commissioned by the Ministry of Education, Culture, Sports, Science and Technology of Japan, by the RFBR (Grant No. 09-02-92482-MNKS_a), EPSRC Grant No. EP/E035728/1, and by the RAS Presidium No. 12 and 27.

[1]M. Roth, A. Blazevich, M. Geissel, T. Schlegel, T. E. Cowan, M. Allen, J.-C. Gauthier, P. Audebert, J. Fuchs, J. Meyer-ter-Vehn, M. Hegelich, S. Karsch, and A. Pukhov, Phys. Rev. ST Accel. Beams **5**, 061301 (2002).
[2]M. Borghesi, D. H. Campbell, A. Schiavi, M. G. Haines, O. Willi, A. J. MacKinnon, P. Patel, L. A. Gizzi, M. Galimberti, R. J. Clarke, F. Pegoraro, H. Ruhl, and S. Bulanov, Phys. Plasmas **9**, 2214 (2002).
[3]S. Kar, M. Borghesi, P. Audebert, A. Benuzzi-Mounaix, T. Boehly, D. Hicks, M. Koenig, K. Lancaster, S. Lepape, A. Mackinnon, P. Norreys, P. Patel, and L. Romagnani, High Energy Density Phys. **4**, 26 (2008).
[4]T. Ditmire, J. W. G. Tisch, E. Springate, M. B. Mason, N. Hay, J. P. Marangos, and M. H. R. Hutchinson, Phys. Rev. Lett. **78**, 2732 (1997).
[5]A. S. Boldarev, V. A. Gasilov, A. Ya. Faenov, Y. Fukuda, and K. Yamakawa, Rev. Sci. Instrum. **77**, 083112 (2006).
[6]Y. Fukuda, A. Ya. Faenov, T. Pikuz, M. Kando, H. Kotaki, I. Daito, J. Ma, L. M. Chen, T. Homma, K. Kawase, T. Kameshima, T. Kawachi, H. Daido, T. Kimura, T. Tajima, Y. Kato, and S. V. Bulanov, Appl. Phys. Lett. **92**, 121110 (2008).
[7]A. I. Magunov, A. Ya. Faenov, I. Yu. Skobelev, T. A. Pikuz, S. Dobosz, M. Schmidt, M. Perdrix, P. Meynadier, O. Gobert, D. Normand, C. Stenz, V. Bagnoud, F. Blasco, J. R. Roche, F. Salin, and B. Yu. Sharkov, Laser Part. Beams **21**, 73 (2003).
[8]T. Nakamura, Y. Fukuda, A. Yogo, M. Tampo, M. Kando, Y. Hayashi, T. Kameshima, A. S. Pirozhkov, T. Zh. Esirkepov, T. A. Pikuz, A. Ya. Faenov, H. Daido, and S. V. Bulanov, Phys. Lett. A **373**, 2584 (2009).
[9]B. L. Henke, E. M. Gullikson, and J. C. Davis, ADNDT **54**, 181 (1993) http://www.srim.org/#SRIM.